Space-Bandwidth Capacity-Enhanced Digital Holography

Applied Physics Express 6 (2013) 022502
http://dx.doi.org/10.7567/APEX.6.022502

Space-Bandwidth Capacity-Enhanced Digital Holography

Tatsuki Tahara[1,2]*, Yasuhiro Awatsuji[1], Kenzo Nishio[3], Shogo Ura[1], Osamu Matoba[4], and Toshihiro Kubota[5]

[1] Graduate School of Science and Technology, Kyoto Institute of Technology, Kyoto 606-8585, Japan
[2] Research Fellow of the Japan Society for the Promotion of Science, Chiyoda, Tokyo 102-7472, Japan
[3] Advanced Technology Center, Kyoto Institute of Technology, Kyoto 606-8585, Japan
[4] Graduate School of System Informatics, Kobe University, Kobe 657-8501, Japan
[5] Kubota Holography Laboratory Corporation, Uji, Kyoto 611-0042, Japan
E-mail: tahara@kit.dj

Received December 3, 2012; accepted January 11, 2013; published online February 5, 2013

We propose a single-shot digital holography in which the space bandwidth available for recording an object wave can be extended in an off-axis configuration. The key points of this technique are utilizing the periodicity of a digital signal and the undersampling, intentionally setting the aliasing to the recorded hologram, and conducting spatial-carrier phase-shifting interferometry and the Fourier transform method. The image quality for both large objects and fine structures can be improved by the keys. The effectiveness of the proposed technique was numerically and experimentally demonstrated. Then, the performance and the optimal angle condition were quantitatively analyzed.

Holography[1)] is a scheme for recording the complex amplitude distribution of an object wave and then reconstructing a three-dimensional (3D) image of an object. A 3D image for any ultrafast physical phenomenon can be captured by holography, and even 3D motion-picture recording of light pulse propagation has been achieved.[2)] Digital holography is a technique for obtaining a hologram by using an image sensor and then reconstructing both a 3D image and quantitative phase distribution by using a computer.[3)] It has been actively researched in the fields of quantitative phase imaging,[4)] microscopy,[5)] object recognition,[6)] and nonlinear imaging.[7)]

However, there is a problem with digital holography in that the quality of the object image is degraded because the 0th-order diffraction wave and the conjugate image become superimposed on the desired image. Single-shot, quantitative 3D imaging without the unwanted images can be achieved by off-axis digital holography using the Fourier transform method,[8)] but most of the space bandwidth (SBW) of an image sensor is discarded to avoid the superimposition in this digital holography without ingenuity. Although parallel phase-shifting digital holography was proposed as a way to solve these problems,[9)] this technique requires a special optical-device and a complicated optical setup.

In this article, we propose space-bandwidth capacity-enhanced (SPACE) digital holography to achieve single-shot, high-quality, and wide-area 3D imaging of dynamic phenomena in an off-axis configuration. The SBW available for recording the object wave is extended by using the periodicity of a digital signal and intentionally setting the aliasing. The unwanted images are removed by spatial-carrier phase-shifting interferometry[10)] and the Fourier transform method.[8)] We conducted numerical simulations and experimented to verify the effectiveness of SPACE, and analyzed the performance and optimal condition of the incident angle of the reference wave quantitatively.

We explain the concept of SPACE digital holography. Figure 1 shows the schematic of SPACE digital holography. The incident angle of the reference wave, which can be either θ_x or θ_y, is introduced to generate the spatial carrier. θ_x or θ_y should be set to be $\sin^{-1}(\lambda/2d)$ to generate fine interference fringes. Here, λ is the wavelength of the optical source used to record a hologram and d is the pixel pitch of

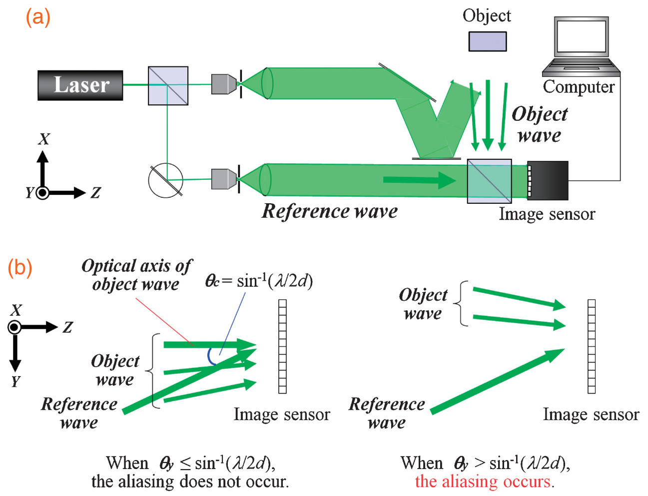

Fig. 1. Schematic of SPACE digital holography. (a) Optical arrangement, (b) relationship between the aliasing and propagation direction of an object wave.

an image sensor. Hereafter, we set θ_y as $\sin^{-1}(\lambda/2d)$ and θ_x to be $0 < |\theta| < \sin^{-1}(\lambda/2d)$. The optimum angle for θ_x is described later. When interference fringes are too fine to be captured by an image sensor, the image sensor cannot recognize the fringes correctly, and an undersampling of the fringes occurs. By setting the angle $\sin^{-1}(\lambda/2d)$, the aliasing occurs according to the propagation direction of the object wave, as shown in Fig. 1(b). As a result, an image sensor records the interference fringe pattern in which the spatial frequencies are modulated by the undersampling. Figure 2 shows the spatial frequency distributions of holograms obtained by a conventional off-axis configuration and SPACE digital holography. We assume that each object wave has an isotropic maximum wavenumber in the in-plane direction in each case. The spectra of the 0th-order wave, the conjugate image, and the object wave are separated according to the spatial carrier. Figures 2(a) and 2(b) show that only the object wave can be extracted by off-axis digital holography when the SBW required for recording the object wave is not so wide in comparison with the SBW of an image sensor. Figure 2(c) shows that the spectrum of the 0th-order wave becomes superimposed onto that of the object wave in the gray-colored area by a conventional

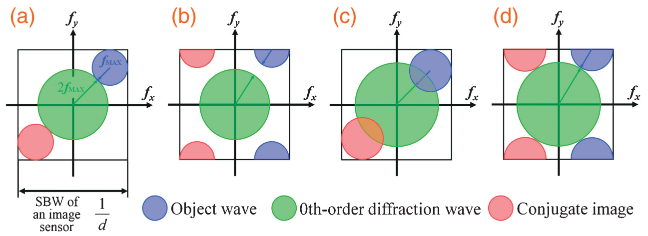

Fig. 2. Spatial frequency distributions of a recorded hologram in the cases where (a), (b) no superimposition of the unwanted images in either digital holography, (c), (d) slight superimposition in the conventional off-axis configuration, but no superimposition in SPACE digital holography. (a) and (c) Those obtained by a conventional configuration and (b) and (d) those obtained by SPACE.

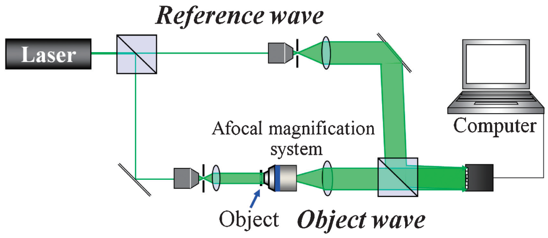

Fig. 3. SPACE digital holographic microscopy adopting an afocal magnification system for numerical simulations.

off-axis configuration, which is caused by the extension of the SBW required for recording the object wave. The spectra of the object wave and the conjugate image, as shown in Figs. 2(b) and 2(d) respectively, become two semicircular shapes in SPACE digital holography. This is due to the periodicity of a digital signal and undersampling. Thanks to adequately setting the spatial carrier, the distance in the spatial frequency domain between the spectrum of the 0th-order wave and that of the object wave is extended. This way, the wide SBW for recording the object wave is available with less superimposition, in comparison with a conventional off-axis configuration. The 0th-order wave and conjugate image are removed by spatial-carrier phase-shifting interferometry[10)] utilizing the spatial carrier generated by the angle $\sin^{-1}(\lambda/2d)$ and the Fourier transform method, respectively. The SBW available for recording the object wave is related to both the resolution and field of view. Thus, SPACE digital holography can do high-quality 3D imaging for both wide areas and fine structures.

We conducted numerical simulations to verify the effectiveness of SPACE digital holography. We numerically simulated digital holographic microscopy adopting an afocal magnification system shown in Fig. 3. A microscopy image of the USAF 1951 test target shown in Fig. 4(a) was set as the amplitude image of the object wave. The wavenumber distribution of the object wave in the in-plane direction was set to be $\sqrt{k_x^2 + k_y^2} \leq \pi/(2d)$. This means that the SBW used for recording the object wave on each axis corresponds to half of the SBW of an image sensor. d, λ, and the distance between the magnified image of the object and an image sensor plane z were 2.2 μm, 532 nm, and 5 mm, respectively. The intensity ratio of the reference wave to the object wave was 1. Object images were reconstructed by the following two techniques: conventional off-axis digital holography with the Fourier transform method,[8)] and SPACE digital holography. Also, we simulated numerically the case where a hologram was obtained by using a low-numerical-aperture (NA) microscope objective and an object image was reconstructed by the conventional off-axis one. The maximum wavenumber of the object wave in the in-plane direction was limited by the objective and superimposition was avoided as shown in Fig. 2(a). Figures 4(b)–4(d) show the object images obtained by the conventional off-axis configuration, the conventional off-axis configuration using a low-NA microscope objective, and SPACE digital holography, respectively. Figure 4(b) shows that the residual 0th-order

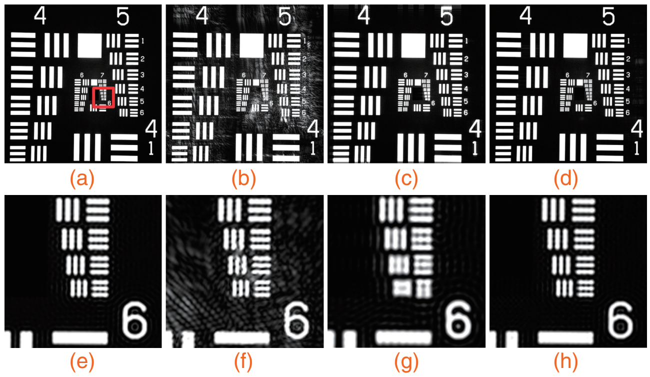

Fig. 4. Microscopic object for numerical simulations and the numerical results. (a) Entire object and images obtained by (b) a conventional off-axis configuration, (c) that using a low-NA microscope objective, and (d) SPACE digital holography. (e)–(h) Each magnified area of (a)–(d), which is indicated by the square in (a).

wave becomes superimposed on the object image while an image mostly free from the unwanted images is reconstructed by SPACE digital holography as shown in Fig. 4(d). Figures 4(e)–4(h) show the magnified areas of the object and the reconstructed images. Although the clear image without the unwanted images was reconstructed by the conventional technique using a low-NA microscope objective, fine structures cannot be reconstructed because of the limit of the spatial information by the objective, as shown in Fig. 4(g). Figures 4(b), 4(c), 4(f), and 4(g) indicate that the removal of the unwanted images and the reconstruction of a large amount of spatial information cannot be simultaneously achieved in the conventional off-axis configuration. In contrast, fine structures of the object are reconstructed with few unwanted images by the extension of the SBW in SPACE digital holography. Thus, the effectiveness of the proposed technique was numerically verified.

We also experimented to demonstrate the single-shot wide-area 3D imaging ability. An optical setup shown in Fig. 1(a) was constructed. A Nd:YVO_4 laser operating at 532 nm was used as the light source. A CMOS image sensor [2592 (H) × 1944 (V) pixels, pixel size: 2.2 × 2.2 μm^2, A/D: 12 bits] was used to record a hologram. This time, we set a cherry blossom as the object and the distance between the object and the image sensor z was 245 mm. Figure 5 shows the photograph of the object and the images reconstructed by both the conventional[8)] and proposed digital holography. Figure 5(b) shows the superimposition of the 0th-order wave on the object image. This superimposition is caused by the fact that the SBW required for

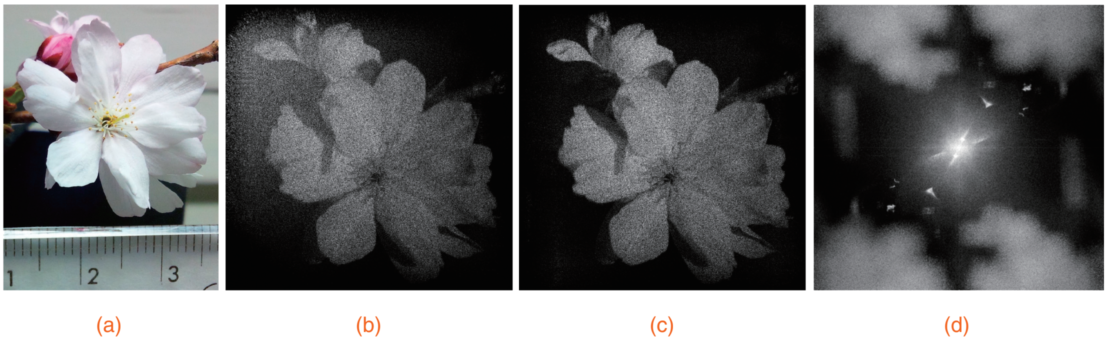

Fig. 5. Object for experiments and experimental results. (a) Photograph of the object, (b) object image obtained by the conventional off-axis configuration, and (c) that obtained by SPACE digital holography. (d) Spatial frequency distribution of the hologram obtained by SPACE.

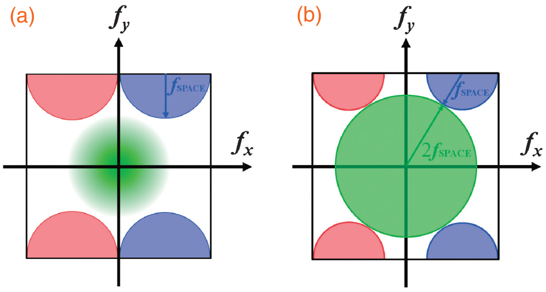

Fig. 6. SBWs available for recording an object wave in SPACE digital holography. Cases where the object wave is (a) weaker and (b) stronger than the reference wave.

recording the object wave is extended when capturing a wide area. Therefore, the unwanted image strongly becomes superimposed in the case of measuring a wide area in the conventional technique. In contrast, a clear image was reconstructed by SPACE digital holography as shown in Fig. 5(c). Figure 5(d) shows the spatial frequency distribution of the hologram recorded by SPACE digital holography. The information of the object wave was separated from the unwanted images. Thus, a high-quality image of a wide area was reconstructed by SPACE digital holography.

We discuss the SBW available for recording the object wave in SPACE digital holography and the optimal angle of θ_x for the maximization of the SBW. Figure 6 shows the three spectra of the proposed technique in the spatial frequency domain. It can be considered that SPACE digital holography is not adversely affected by the 0th-order wave in the case where the object wave is weaker than the reference wave. Reference 11 indicates that the high spatial-frequency component of the 0th-order wave can be almost negligible in the case above. Then, the numerical results show that a much clearer image can be reconstructed by SPACE digital holography in comparison with the conventional off-axis configuration. Therefore, in the case above, the spectrum of the 0th-order wave can be regarded as negligible, and the maximum spatial frequency utilized to record the object wave f_{SPACE} is extended to $1/(4d)$. From the schematic of the spectrum, in the case where the intensity of the object wave is higher than that of the reference wave, f_{SPACE} is geometrically calculated and given by

$$f_{\mathrm{SPACE}} = \frac{\sqrt{17}-1}{16d} \approx \frac{0.195}{d}. \tag{1}$$

This equation means that in the cases above, the SBWs of SPACE digital holography are extended 1.56 and 1.22 times in comparison with the conventional one.[8] Subsequently, the optimal angles of θ_x in these cases are $\sin^{-1}(\lambda/4d)$ and $\sin^{-1}[(9-\sqrt{17})\lambda/16d]$, respectively.

We proposed and experimentally demonstrated SPACE digital holography. The proposed technique does not require either a numerical filter requiring the intensity distribution of only the reference wave or an iteration process for removing the unwanted images. Therefore, single-shot 3D imaging with a wide field of view can be achieved with simple image processing and a simple optical system. Note that the visibility of fine interference fringes decreases when the fill factor of each photo detector in the image sensor is close to 100%.[12] It is a future work to compensate the influence caused by the decrease of the visibility. This technique has the potential for high-quality, quantitative, 3D imaging for dynamically moving objects, as well as for the application to microscopy, polarization imaging in 3D space, 3D multispectral imaging, object recognition, and other 3D imaging applications.

Acknowledgments We appreciate Kris Cutsail and Mwangi Job Kihungi for checking the English grammar of this article. This study was partially supported by a Grant-in-Aid for JSPS Fellows from the Japan Society for the Promotion of Science (JSPS), and by the Funding Program for Next-Generation World-Leading Researchers GR064 of JSPS.

1) D. Gabor: Nature **161** (1948) 777.
2) T. Kubota, K. Komai, M. Yamagiwa, and Y. Awatsuji: Opt. Express **15** (2007) 14348.
3) J. W. Goodman and R. W. Lawrence: Appl. Phys. Lett. **11** (1967) 77.
4) Y. Ichioka and M. Inuiya: Appl. Opt. **11** (1972) 1507.
5) J. Rosen and G. Brooker: Nat. Photonics **2** (2008) 190.
6) E. Tajahuerce, O. Matoba, and B. Javidi: Appl. Opt. **40** (2001) 3877.
7) K. Shi, H. Li, Q. Xu, D. Psaltis, and Z. Liu: Phys. Rev. Lett. **104** (2010) 093902.
8) M. Takeda, H. Ina, and S. Kobayashi: J. Opt. Soc. Am. **72** (1982) 156.
9) Y. Awatsuji, M. Sasada, and T. Kubota: Appl. Phys. Lett. **85** (2004) 1069.
10) T. Tahara, Y. Shimozato, Y. Awatsuji, K. Nishio, S. Ura, O. Matoba, and T. Kubota: Opt. Lett. **37** (2012) 148.
11) J. W. Goodman: *Introduction to Fourier Optics* (Roberts & Co., Englewood Cliff, NJ, 2005), 3rd ed., Chap. 9.
12) T. M. Kreis: Opt. Eng. **41** (2002) 771.